STUDY ON ANTI-ERROSION OF O'-SIALON/BN AND O'-SIALON/ZrO$_2$ COMPOSITES IN MOLTEN STEEL AND SLAG

H. BAO   Q. ZHEN   W. C. LI

University of Science and Technology Beijing, Beijing 100083, P. R. China

ABSTRACT: Erosions of O$'$-Sialon/BN in molten steel and O$'$-Sialon/ZrO$_2$ in protective slag of continuous casting were investigated in present work. According to experimental results and theoretical analysis, erosion kinetics of the O'-Sialon/BN in molten steel was controlled by two steps: the first one is controlled by a chemical reaction taking place on the interface; the second one is controlled by diffusion through boundary layers. The O'-Sialon/ZrO$_2$ composites had good erosion resistance to continuous casting protective slag because the solubility of ZrO$_2$ in silicate melt is limited and the increment of ZrO$_2$ content will prevent O'-Sialon from reacting with dissolved CO and other components in slag so that the erosion resistance of the O'-Silon/ZrO$_2$ against molten slag was improved.

Key words: O'-Sialon/BN, O'-Sialon/ZrO$_2$, Erosion resistance, Fractal

1. INTRODUCTION

O$'$-Sialon-containing refractory materials have many superior properties to be used in continuous casting. Both of the O$'$-Sialon/BN used as a break ring for Horizontal Continuous Casting (HCC) and the O'-Sialon/ZrO$_2$ used as a submersed nozzle have excellent thermal shock resistance, high temperature strength and oxidation resistance[1-6]. O$'$-Sialon/BN also has certain machine-shaping ability so that different parts with precise size can be made from the composites[2] while the O'-Sialon/ZrO$_2$ has an adhesion resistance against alumna to prevent Al$_2$O$_3$ from heeling and blocking the nozzle. On the other hand, under actual sever service conditions with molten steel and slag co-exist at high temperatures, it might be believed that the break ring would be eroded by molten steel and the submersed nozzle would react with protective slag. However, little work was reported in literature about erosion resistance of O$'$-Sialon/BN and O'-Sialon/ZrO$_2$. The metal erosion resistance of O$'$-Sialon/BN and the slag erosion resistance of O'-Sialon/ZrO$_2$ are studied in this work.

2. EXPERIMENTAL PROCEDURE

Erosion experiments were carried out in a molybdenum wire furnace with temperature controlled by a PID controller. The experimental apparatus is shown in Figure 1.

For erosion resistance of O$'$-Sialon/BN in molten steel, O$'$-Sialon/BN with 70mass% BN were synthesized by hot pressing and shaped into test bars with dimensions of 40×3×4mm^3. The surfaces of the test bars were rubbed and polished before use. Firstly, carbon steel was melted and maintained at 1600□. Then all the test bars were put into the melted steel and then were taken out one by one after 5, 10, 20, 30, 45, 60 minutes respectively. During the experiments, N$_2$ was blown into the furnace from bottom to prevent oxidation of steel. N$_2$ was also blown into crucible from the top of the furnace to simulate actual service conditions.

For erosion experiments of O'-Sialon/ZrO$_2$ composites in protective slag, the O'-Sialon/ZrO$_2$ with ZrO$_2$ contents from 10% (Z1), 20% (Z2), 30% (Z3) to 40% (Z4) respectively, was synthesized by pressure free sintering. Pure ZrO$_2$ was also used in the

erosion study in order to make comparison. The dimension of the test bars was $40\times10\times10mm^3$. Their surfaces were polished before being put into furnace. The steel/slag phases should exist simultaneously in order to simulate actual service conditions of continuous casting. The temperature of molten steel is 1550□ and the average temperature on the boundary between protective slag and molten steel is about 1450□. Nitrogen gas was blown in to simulate turbulence in the melts during the experiment. At the maintained temperature, all the test bars with different ZrO_2 contents were put into the molten slag and were then taken out after 40 minutes. The composition of the protective slag for erosion test is shown in table 1.

Finally, the eroded samples were cut into pieces. The cross-sectional surfaces of test bars were polished and coated with a carbon film for SEM observation.
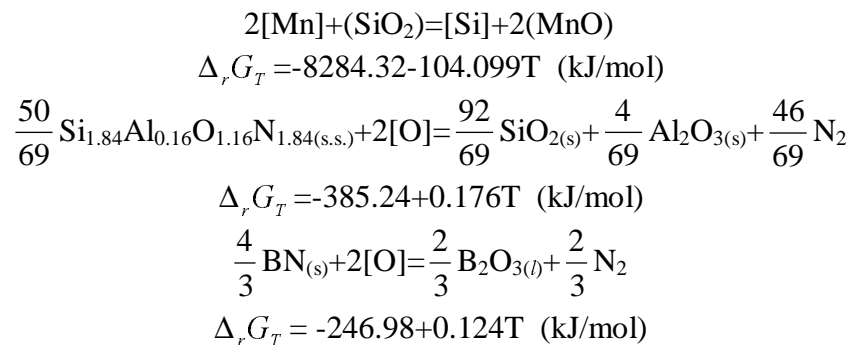
3. RESULTS AND DISCUSSION
3.1 METAL EROSION RESISTANCE OF THE O′-SIALON/BN COMPOSITIONS
## 3.1.1 RESULTS

Erosion depth vs. time for O′-Sialon/BN samples in molten steel at 1600□ is shown in figure 2. It can be seen from the figure 2 that the curve changes in a linear way at the beginning and then the erosion rate slowed down in a parabola way after 20 minutes.

Figure 3 indicates that the samples changed a little at 5 minutes (Fig.3(a)); the eroded surface became uneven after 20 minutes but the erosion layer is not more than 10μm (Fig.3(b)). The eroded surfaces become more concave-convex with erosion time last and thickness of eroded layer increased (Fig.3(c)~(d)).

Figure 4 shows cross-sectional microstructure of eroded layer of sample after 60 minutes of erosion. It can be seen from figure 4 that the thickness of the eroded layer is not more than 50μm; the structure of exterior layer close to molten steel is loosened. There are some erosion channels there while the structure of inner layer close to matrix is compact. According to thermodynamic calculation, the [Mn] in molten steel may react with SiO_2 among grains to generate a low-melting slag of MnO-SiO_2-Al_2O_3[7, 8]. The slag will permeate in grain boundaries to form some erosion channels, which change the structure of samples and make them dissolved. In the meantime, the [O] in molten steel react with O′-Sialon to generate SiO_2 and Al_2O_3[7]. The SiO_2 will be eroded further by molten steel. Therefore, it is believed that the erosion of O′-Sialon-BN samples is a procedure of reaction and solution:

$$2[Mn]+(SiO_2)=[Si]+2(MnO)$$
$$\Delta_r G_T = -8284.32-104.099T \text{ (kJ/mol)}$$
$$\frac{50}{69}Si_{1.84}Al_{0.16}O_{1.16}N_{1.84(s.s.)}+2[O]=\frac{92}{69}SiO_{2(s)}+\frac{4}{69}Al_2O_{3(s)}+\frac{46}{69}N_2$$
$$\Delta_r G_T = -385.24+0.176T \text{ (kJ/mol)}$$
$$\frac{4}{3}BN_{(s)}+2[O]=\frac{2}{3}B_2O_{3(l)}+\frac{2}{3}N_2$$
$$\Delta_r G_T = -246.98+0.124T \text{ (kJ/mol)}$$

There are many white BN grains in the eroded layer, as shown in Figure 5. This is because that the liquid steel has very big wetting angle with BN and BN does not react easily with steel. The BN react with dissolved oxygen in the steel to form B_2O_3 which will then react with Al_2O_3 in O′-Sialon to form $9Al_2O_3\cdot2B_2O_3$[7]:

$$9Al_2O_3 + 2B_2O_3 = 9Al_2O_3 \cdot 2B_2O_3$$
$$\Delta_r G^{\circ}_{1600K} = -189.02 \quad (kJ/mol)$$
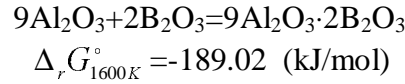
The $9Al_2O_3 \cdot 2B_2O_3$ can prevent BN from further oxidation. Therefore, surplus BN grains will be accumulated in the eroded layer after glass phase and O′-Sialon were eroded.

3.1.2   EROSION KINETICS

The erosion of O′-Sialon/BN samples in molten steel is a solid-liquid reaction, including procedure of intruding of components within molten steel into the composites and interface chemical reaction. The erosion procedure includes two stages: 1) earlier stage —— interface chemical reaction controlled, and 2) final stage —— diffusion controlled.

1. INTERFACE CHEMICAL REACTION

The reaction of O′-Sialon/BN samples with molten steel contains three steps: 1) the components in molten steel diffuse to surface of sample through liquid-solid boundary; 2) the components in molten steel react with glass phase and O′-Sialon in the composites; 3) low-melting phase formed from the reaction diffuses in liquid-solid boundary. The reaction speed can be express as follows:

$$x = kt \tag{1}$$

Here,

$$k = \frac{k_c' C}{P_1 (1-R) \rho}$$

where C is the concentration of component that participates in the reaction within molten steel; k_c' is the constant of reaction rate; P_1 is the volume percentage of the O′-Sialon phase in composites; ρ is the bulk density of the composites; R is a ratio of dissolved materials to total materials in the erosion layer.

Equation 1 shows that the curve of erosion depth vs. time is linear. The erosion rate equation is derived by regression from the figure 2 as below:

$$= 0.02 \quad \text{(correlation coefficient } R=0.99919) \tag{2}$$

2. DIFFUSION

After a certain period of erosion, the thickness of eroded layer increased to a considerable level. Therefore, diffusion path of reactant and product become longer than before and diffusion resistance increased. At this time, diffusion becomes restrictive step. The reaction speed can be express as:

$$x^2 = k_D t \tag{3}$$

where

$$k_D = \frac{2CD}{P_1 (1-R)^2 \rho}$$

where D is diffusion coefficient in erosion layer for reacting component.

Equation (3) shows that erosion rate is in accord with parabolic equation at final stage. From the figure 2, the erosion rate equation was derived as below:

$$x^2=0.0337t \quad \text{(correlation coefficient R=0.99705)} \quad (4)$$
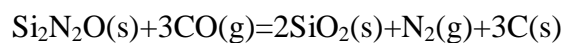
3. FRACTAL OF EROSION INTERFACE

Figure 6 shows results of binary imaging and fractal curve of erosion interface from figure 3. The fractal dimension can be measured with FDCP program in our laboratory. It can be seen from figure 7 that the curve of the fractal dimension vs. time is in accord with experimental results.

All the analyses show that the erosion of O′-Sialon/BN composites in molten steel is somewhat self-protected. Because the [Mn] in molten steel reacts with only a few glass phases in samples to generate a low-melting slag and the [O] in molten steel reacts with O′-Sialon at the same time. However, erosion effect of molten steel to BN grains is limited so BN grains will accumulate in erosion layer and form a thicker and thicker diffusion layer, which will impede erosion reaction of samples in molten steel.
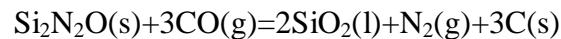

3.2 EROSION OF O'-SIALON-ZrO₂ IN PROTECTIVE SLAG

Figure 7 and 8 show the SEM microstructures on crossing sections of the O'-Sialon-ZrO_2 composites and the pure ZrO_2 samples. The eroded samples contain three layers: eroded slag layer, transition layer and un-eroded original layer. For O'-Sialon-ZrO_2 composite, the eroded slag layer can be divided into two layers. The outer layer is about 200μm, containing many air bubbles. The inner layer is about 200~400μm, which is more compact than the outer layer. The depth of the transition layer in the middle reduced with the increment of ZrO_2 content. For ZrO_2 sample, the slag layer is very thin, which indicates that the ZrO_2 has good resistance ability against to slag erosion. Because the solubility of ZrO_2 in silicate melt is limited, the increment of ZrO_2 will prevent O'-Silon from reacting with dissolved CO and other components in the slag so that the slag resistance ability for the O'-Silon/ZrO_2 composites can be improved. The EDS analysis indicates that the Ca erosion for Z1 sample is deeper than that for Z4. Because the melting point and viscosity of CaF_2 is very low, Ca permeating into samples should be in form of CaF_2. On the other hand, it is believed that the protective slag cannot react with ZrO_2 to form a low-melting compound, so ZrO_2 grains remained in the transition layer close to internal matrix when O'-Sialon grains have reacted with slag. It made apparent that the viscosity of transition layer increased and prevented Ca from diffusing in transition layer.
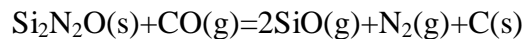
In erosion experiment, O_2 in air can dissolve little in slag because of the protection of carbon-rich layer and solid protective slag. Another oxygen source may be from [O] in molten steel, which enter slag with ferric oxide. Therefore, carbon was oxidized mainly to form CO. The CO can destroy the oxide layer around O'-Sialon and react further with it[7,8]:

$$Si_2N_2O(s)+3CO(g)=2SiO_2(s)+N_2(g)+3C(s)$$
$$\Delta^{\circ}=-868.06+0.52T \text{ (kJ/mol)}$$
$$Si_2N_2O(s)+3CO(g)=2SiO_2(l)+N_2(g)+3C(s)$$
$$\Delta^{\circ}=-859.03+0.51T \text{ (kJ/mol)}$$
$$Si_2N_2O(s)+CO(g)=2SiO(g)+N_2(g)+C(s)$$

$$\Delta \quad ^\circ =-466.02-0.14T \ \ (kJ/mol)$$

Bubbles in slag layer are caused by chemical reaction between O'-Sialon and CO. the Sample's structure became loose because of decomposition of O'-Sialon. In addition, the eutectic temperature of CaO-SiO_2-Si_3N_4 system is below 1450□ according to the phase diagram of CaO-SiO_2-Si_3N_4. Other components in the slag will further decrease the eutectic temperature. Therefore, the samples with more O'-Sialon will be eroded by liquid phase under experimental condition.

The fractal study of eroded interfaces of Z1, Z4 and ZrO_2 (Figure 9) shows that the fractal dimensions increase slightly with ZrO_2 content. The reason is that the increment of ZrO_2 content will reduce CO migration rate in samples and therefore prevented CO from reacting with O'-Sialon. This phenomenon accords with the experimental results.

4. CONCLUSION

1. The main reasons for O′-Sialon-BN erosion are as follows: first, a chemical reaction takes place between [Mn] in molten steel and SiO_2 in glass phase among grains; second, MnO-SiO_2-Al_2O_3, which is a low-melting-point slag and product of the reaction, permeates in grain boundaries and forms some corrosion channels. Meanwhile, [O] in molten steel would react with O′-Sialon to form SiO_2 and Al_2O_3. Then, the SiO2 will be eroded. BN is hard to react with molten steel. Therefore, BN grains will accumulate in eroded layer to form a thick diffusion layer gradually, which impedes erosion reaction of samples in molten steel.
2. The erosion of O′-Sialon-BN samples in molten steel includes two stages: 1) earlier stage —— interface chemical reaction, 2) final stage —— diffusion. The erosion rate can be express as:
    Interface chemical reaction-controlled stage: $x=0.02t$
    Diffusion-controlled stage: $x^2=0.0337t$

    In addition, the variance of erosion interface fractal dimension with time accords with the erosion mechanism of samples in molten steel.
3. Erosion of O'-Silon-ZrO2 in protective slag is due to the reaction of O'-Sialon with CO.
4. The ability for O'-Silon-ZrO_2 preventing erosion by protective slag increases with ZrO2 content. The reason is that ZrO_2 prevented O'-Sialon from reacting with CO .

5. ACKNOWLEDGEMENT

Reference

[1] Gu Peizhi, Lee Wenhong, Sintering, Properties and Application of Sialon-ZrO_2 and Sialon-ZrO_2-BN Fiber Composites, High Tech. Ceramics, Edited by P. Vincenzini, Elsevier Science Publishers B. V., Amsterdam, Printed in the Netherlands, (1987), 2725-2733
[2] Qiang Zhen, Wenchao Li, Recent Development of the Break Ring for the Horizontal Continuous Casting, Refractory Materials, Vol.32, No.4, (1998), 234-237
[3] Richard Larker, Reaction Sintering and Properties of Silicon Oxynitride Densified by Hot Isostatic Pressing, J. Am. Ceram. Soc. Vol.75, No.1, (1992), 62-66
[4] D. B. Hoggard, H. K. Park, O′-Zircomia and its refractory application, Ceramic Bulletin, Vol.69, No7, (1990), 1163-1166
[5] Y. B. Cheng, D. P. Thompson, Densification of Zirconia-containing Sialon Composites by

Sm$_2$O$_3$, J. Mat. Sci., Vol.28, (1993), 3097-3102

[6] V. M. Sglavo, R. D. Maschio, G. D. Soraru, Fabrication and Characterization of Polymer-derived Si$_2$N$_2$O-ZrO$_2$ Nano-composite Ceramics, J. Mat. Sci. 28, (1993), 6437-6441

[7] JANAF "Thermochemical Tables", 3rd Edn, American Chemical Society and American Institute of Physics for NBS,1986

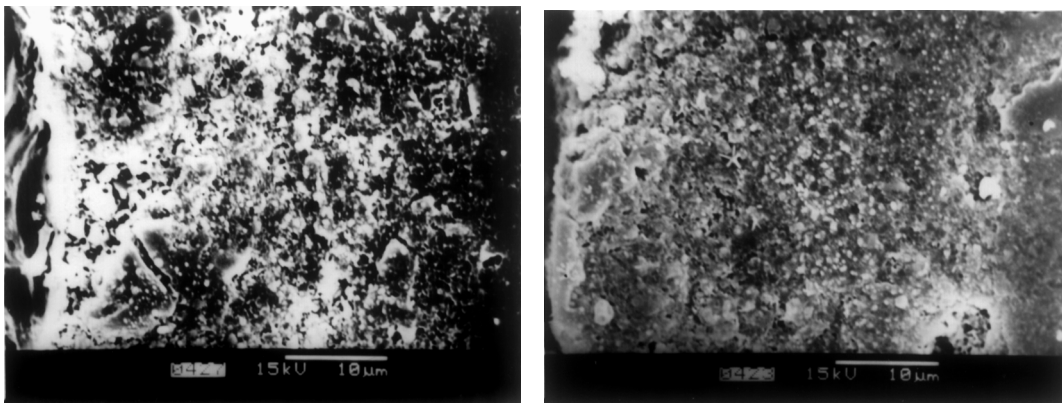[8] Shou-kun Wei, Thermodynamics of Metallurgical process, Shanghai Press of Science and Technology, Shanghai, China, 1980
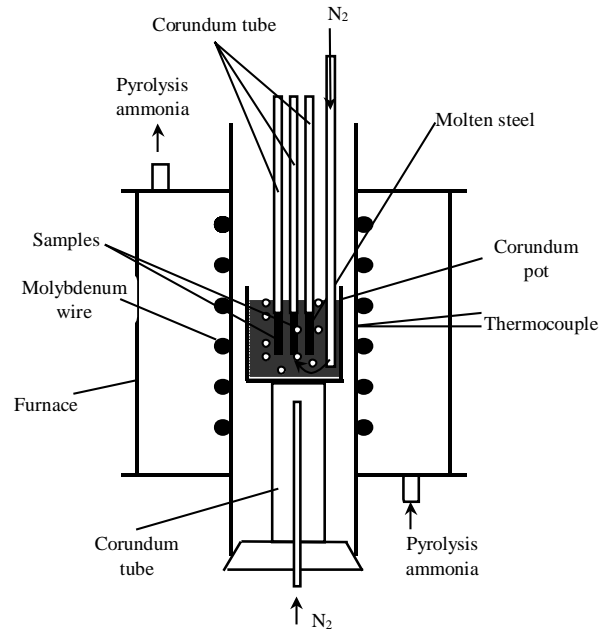
Figure 1   Experimental apparatus for erosion test
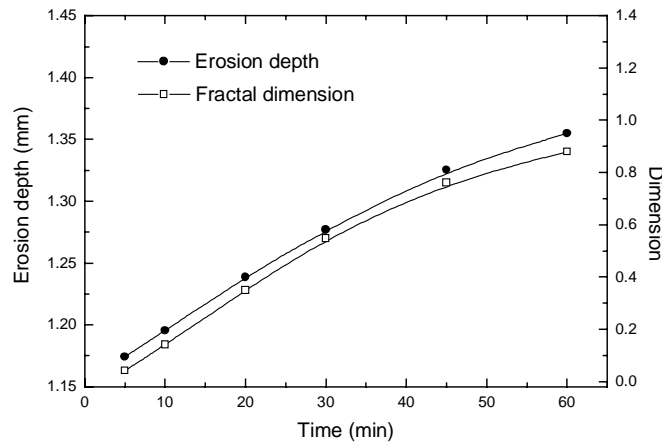
Figure 2   Curve of Erosion depth and fractal dimension vs. time for O′-Sialon-BN samples at 1600□

(a) 5min   (b) 20min

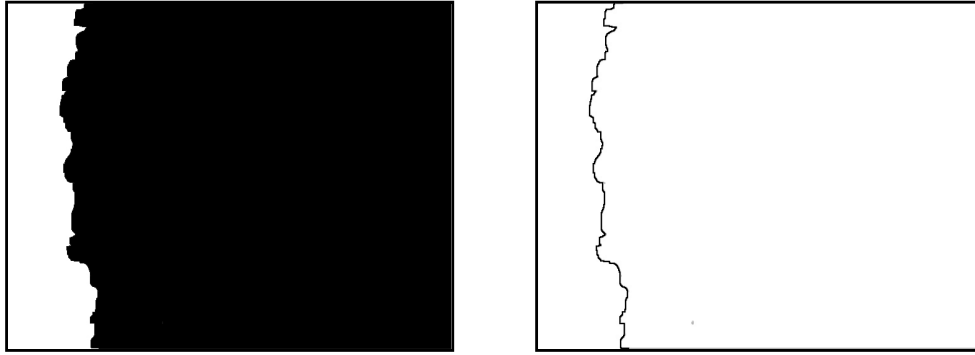(c) 45min   (d) 60min
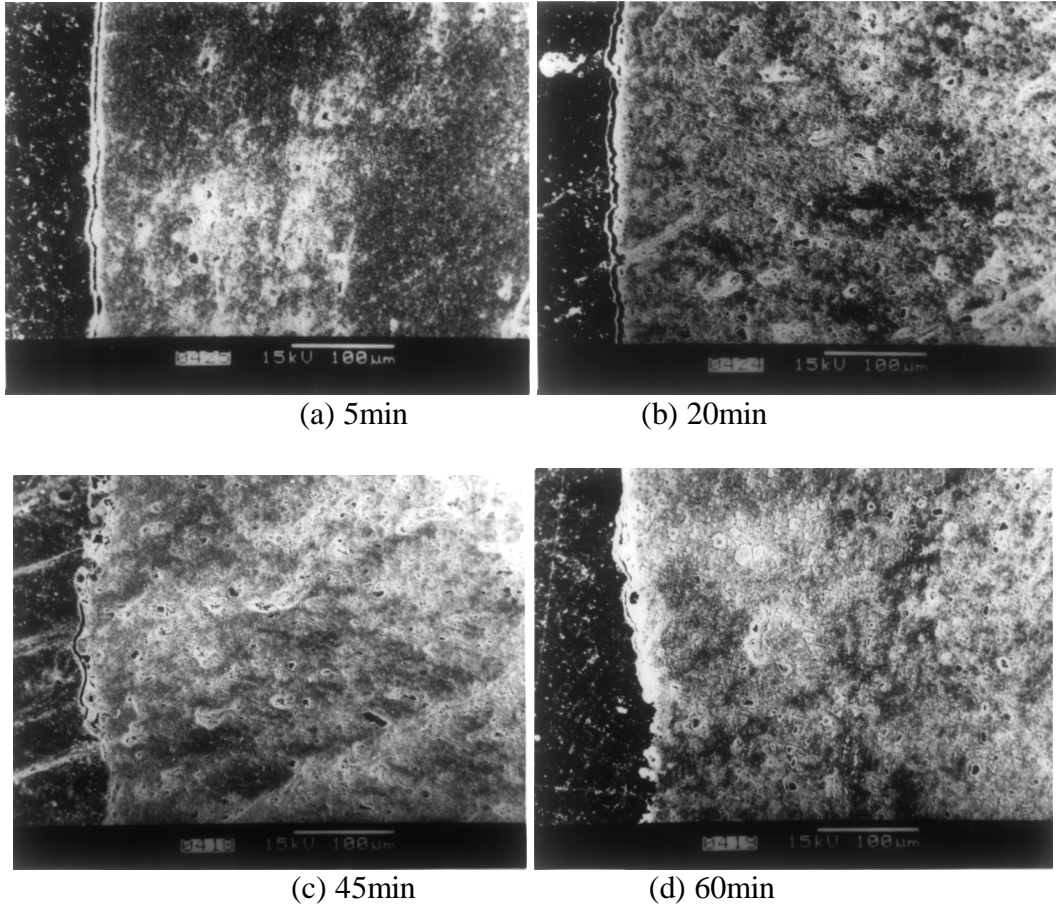
Figure 3   SEM micrograph of BN-O′-3 samples after erosion

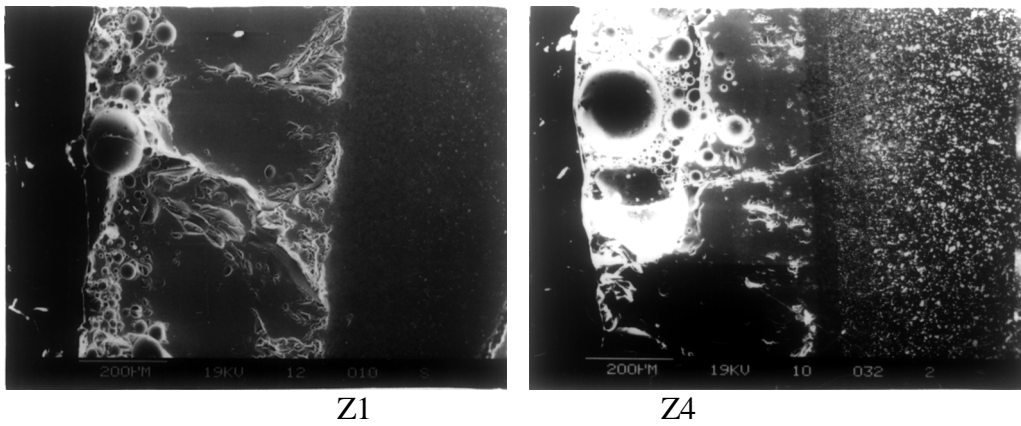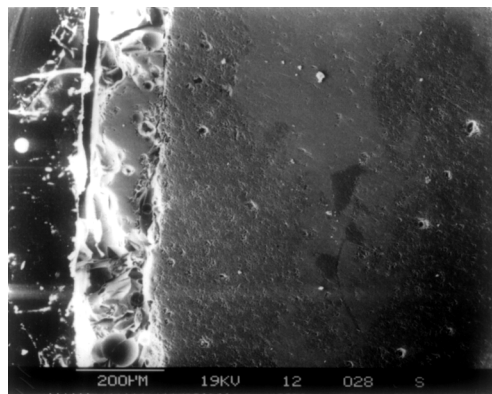**Figure 4   Erosion channels in eroded layer**   **Figure 5   Aggregation of BN**
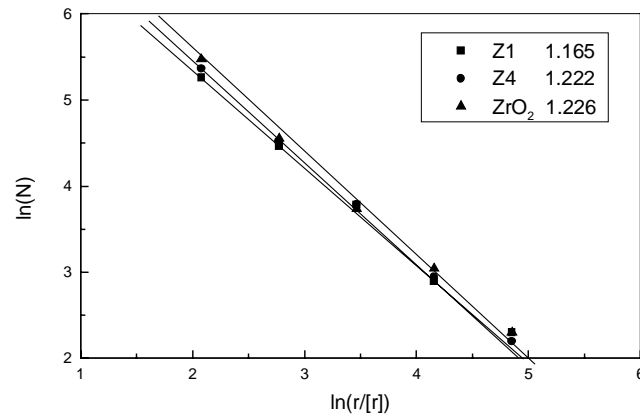
Figure 6   Binary Image and fractal curve

Z1   Z4

Figure 7   Sectional SEM microstructure of O'-Sialon-ZrO$_2$ samples

Figure 8   Sectional SEM microstructure of ZrO$_2$ samples

Figure 9 Fractal dimensions of eroded interface for different ZrO$_2$ contents (erosion time 40min)

Table 1 Composition of protective slag for erosion test

Composition	SiO_2	Al_2O_3	CaO	MgO	Fe_2O_3
mass%	35.5	2.5	34.9	0.6	2.5
Composition	Na_2O	F_2	C	MnO	-
mass%	5.1	4.8	7.7	0.05	-